

OPTICAL FIBER FAILURE PROBABILITY PREDICTIONS FROM LONG-LENGTH STRENGTH DISTRIBUTIONS

G. S. Glaesemann

Corning Incorporated
Corning New York

Abstract

Strength data from a recently developed apparatus for measuring long-length fiber strength distributions are analyzed in terms of proof test theory for truncated distributions. Data are fitted using Weibull statistics and scaled for bending and tensile lengths ranging from 1 meter to 100 kilometers. Most tensile applications require strength data near the proof stress level. For failure probability levels less than 1×10^{-5} most bending applications need be concerned with flaws near the proof stress level.

Introduction

A schematic of a 1986 strength distribution of 16.5 kilometers of titania-doped silica-clad fiber proof tested to 50 kpsi (345 MPa) is shown in Figure 1.¹ Observe that after testing nearly 17 kilometers of fiber the distribution lacks flaws that are of the greatest reliability risk for most applications namely those near the proof stress level. For the purposes of reliability prediction near the proof stress level much more fiber must be tested. Also the amount of time required to manually create multi-kilometer strength distributions using common industry test methods makes the creation of such distributions costly.

The purpose of this paper is to present a recently developed technique for measuring the strength distribution near the proof stress level and to examine how one might use these data for making reliability predictions.

Creating a Long-Length Strength

Distribution

A new fiber strength testing method was recently developed for obtaining data on many kilometers of fiber in a more timely fashion.² It is believed that this test method will enable engineers to better assess the failure probability of flaws near the proof stress level. As shown in Figure 1, 95% of the flaws on 20 meter gauge lengths have strengths greater than 500 kpsi (3500 MPa) and therefore do not present a reliability risk for long-length applications. The approach taken in the development of a long-length strength distribution was to avoid testing the strong flaws to failure. This was accomplished by loading fibers during tensile testing to a maximum load below the high strength region as shown schematically in Figure 2, where the maximum load during testing is set to break all flaws below 400 kpsi (2800 MPa) and pass those that are stronger.

A complete description of the operation of the equipment is given in reference 2 and only a brief description will be given here. The test apparatus is shown schematically in Figure 3 and consists of a proof testing machine for paying out fiber into the gauge length under low loads. The gauge length consists of 20 meters of fiber which starts at point A on the payout tractor travels around a remote pulley assembly and back to point B on the take-up tractor. The pulley assembly consists of a pulley mounted on a load cell both of which are attached to a pneumatic slide. Fiber is payed out under low load into the gauge length after which the pulley assembly moves on the slide and the fiber is loaded to a predetermined maximum load level. As soon as the maximum load is reached the pulley returns to its original position. The load is carefully monitored during the entire load pulse and if failure occurs the breaking load is recorded. Typical load pulses are shown in Figure 4 for fiber that passes and fails the test. If the fiber passes the load pulse test another 20 meter length is indexed into the gauge length and the load pulse is repeated. The loading and unloading rates are in the 200 to 400 kpsi/s (1400 to 2800 MPa/s) range and therefore the probability of subcritical crack growth during testing is high. Using the above apparatus 386 kilometers of titania-doped silica-clad fiber^{4,5} proofed to 50 kpsi (350 MPa) were tested to a maximum stress level of 350 kpsi (2450 MPa) in approximately 4 weeks. All testing was carried out under ambient conditions (20°C, 60% RH). The number of recorded failures below 350 kpsi (2450 MPa) was 106 out of a total 19,300 individual 20 meter tests. The failure probability, F, was assigned to each fiber failure using the median rank method,

$$F = \frac{(I-0.3)}{(J+0.4)} \quad (1)$$

where I is the fiber rank ranging from 1 for the weakest to 106 for the strongest fiber, and J is the total number of tests; namely, 19,300. The data are shown in Figure 5 as a Weibull plot of $\ln \ln(1/(1-F))$ versus $\ln \sigma_f$, where σ_f is the fracture strength. The upper end of the strength distribution stops at the maximum stress level of 350 kpsi, as planned, and the lower end extends to a stress level slightly above the proof stress of 50 kpsi (350 MPa). The above data demonstrate the capability of obtaining multi-kilometer strength distributions in a relatively short period of time.

The theoretical shape for inert strength distributions of proof tested specimens is shown in Figure 6 from reference 3. The pre-proof distribution has a constant slope m. Flaws away

from the proof stress are unaffected by the proof stress and are shown to follow the pre-proof distribution. Those that grow subcritically during proofing have a post-proof slope of $n-2$, where n is the well known fatigue susceptibility parameter from the power law crack velocity model. Finally the distribution is truncated near the proof stress level as indicated by a vertical line. For fast unloading rates the truncation strength is no less than 90% of the proof stress.³

The distribution in Figure 5 differs from the theoretical distribution in that our testing demonstrates subcritical crack growth due to a fatigue environment. In the case where fatigue occurs during strength testing, the truncation strength level will be less than the proof stress, simply because flaws that just pass the proof stress will grow during subsequent strength testing and fail at a stress level below the proof stress. The flaws in the $(n-2)$ slope region will, after crack growth during the strength test, end up with a slope $n+1$.⁶ The data in Figure 5 are linear above the 125 kpsi (875 MPa) stress level with a slope, m , of approximately 2. Below 125 kpsi (875 MPa), the data indicate the transition to a higher slope region prior to truncation shown in Figure 6. However, too few flaws were obtained in this region to accurately determine where a slope of $n+1$ begins, obviously, many more kilometers of data are needed.

Predictions from long-length strength distributions

Optical fibers in the field experience a variety of stress conditions over different fiber lengths. For example, in splice enclosures, relatively short lengths of fiber are subjected to bending; however, considering the number of splice enclosures involved, hundreds and even thousands of meters of fiber are under stress. In this common situation it is important to determine which flaws pose the greatest risk to mechanical reliability. For applications involving kilometers of fiber under low stress, it is common to treat the fiber as if it were no stronger than the proof stress level. However, as fiber comes closer to the home, it is expected to have greater mechanical reliability, thereby, requiring the knowledge and accountability of flaw distribution at and above the proof stress level. Since measured tensile strength distributions typically use lengths that do not match those deployed in service or model loading configurations such as bending, one must scale the distribution to the length and loading configuration appropriate for a given application.

Weibull's cumulative failure probability distribution has found wide applicability for describing the dependence of strength on size. The failure probability at an applied stress is given by,^{7,8}

$$F = 1 - \exp \left[- \int_0^{\sigma} \left(\frac{\sigma}{\sigma_0} \right)^m \frac{dA}{A_0} \right] \quad (2)$$

where m is the Weibull slope, A is the surface area under stress σ , and A_0 is the surface area corresponding to the characteristic strength σ_0 .

Tensile Loading.

For the case of uniaxial tensile loading, the stress at failure is distributed uniformly over the cross section, $\sigma = \sigma_f$, and $dA = r dl d\theta$ where l is the fiber length, r is the fiber radius and θ is the angle as shown in Figure 7. Substituting these values into Eq. (2) yields,

$$F = 1 - \exp \left[- \int_0^{l_t} \left(\frac{\sigma_f}{\sigma_0} \right)^m \frac{2\pi r dl}{A_0} \right] \quad (3)$$

where l_t is the total length in tension. Integration yields the probability of length l_t failing at stress σ_f ,

$$F = 1 - \exp \left[- \left(\frac{\sigma_f}{\sigma_0} \right)^m \frac{2\pi r l_t}{A_0} \right] \quad (4)$$

Thus, Eq. (4) can be used to scale the data for gauge length of area A_0 and characteristic strength σ_0 , to lengths l_t . For l_t equal to the test length, $A_0 = 2\pi r l_t$ and Eq. (4) simplifies to the more familiar Weibull form,

$$F = 1 - \exp \left[- \left(\frac{\sigma_f}{\sigma_0} \right)^m \right] \quad (5)$$

The usefulness of this distribution is that it can be transformed into a linear format as,

$$\ln \ln \left(\frac{1}{1-F} \right) = m \ln \sigma_f - m \ln \sigma_0 \quad (6)$$

where m is the Weibull slope and $-m \ln \sigma_0$ is the intercept.

Recall that data in Figure 5 are plotted in terms of $\ln \ln(1-F)$ versus $\ln \sigma_f$ according to Eq. (6); however, as previously observed, the data are not linear, but rather has a characteristic curvature associated with a truncated distribution.³ Theoretical models for curved distributions are significantly more complex than Eq. (4), and the scaling of such distributions is justified. However, here we take a more pragmatic approach that simplifies scaling significantly, especially in the case of bending.

The distribution in Figure 5 is not extensive enough to attain the theoretical slope of $n+1$; so, for discussion purposes, ranks 1 to 15 were fit to Eq. (6) yielding a slope of approximately 5. Similarly, ranks 15 through 106 were fit to Eq. (6) yielding a Weibull slope of 1.7. The composite distribution is shown in Figure 8. The Weibull parameter σ_0 for each portion of the distribution is also given in Figure 8. Using Eq. (4), where A_0 is the total area for 20 meter test lengths and 62.5 μm glass radius, the composite distribution is scaled to a range of new lengths l_t in Figure 9. Note again that these distributions are degraded following proof testing due to crack growth during strength testing. As expected, the failure probability for each strength level is increased as the in-service length increases. Also note that the shift is slightly greater for the region of the distribution with lower m value. Conversely, as the in-service length decreases, the probability of encountering a flaw near the truncation strength also decreases. However, for a typical failure probability

requirement of 1×10^{-5} , the predicted distribution shows that even applications using only 1 meter lengths in tension need be concerned with flaws below the 600 kpsi (4200 MPa) "high strength" region shown in Figure 1. For stressed lengths 100 kilometers and greater, Figure 9 shows that reliability designs should be focused primarily on flaws near the proof stress level. The data in Figure 9, when matched with a given application, will also help focus on the type of data needed for reliability determinations.

Bending.

The surface tensile stress due to bending of fiber also is a reliability concern, since large stresses are easily generated. However, bending places a considerably smaller area under stress compared to uniaxial tension, due to the fact that only half of the fiber surface is under tensile loading (Figure 10), and the stress distribution over that surface is highly nonuniform. Therefore, it is important to determine what portion of the strength distribution is of concern for a given bend application.

The simplest bending situation is where the entire fiber length in bending experiences a constant bend radius. The Weibull scaling laws for the more complex case of 2-point bending have already been derived by Matthewson et. al.,⁹ and therefore, the analysis here will follow their form and notation.

The surface tensile stresses generated by fiber bending are dependent entirely on the bend configuration. The stress, σ , is zero at the neutral axis, $\theta=0$, and reaches a maximum at $\theta=\pi/2$; see Figure 7. The well known relationship between stress, σ , and the bend radius R is given by,

$$\sigma = \frac{r \sin \theta}{R} E \quad (7)$$

where r is the fiber radius and E is its Young's modulus. Young's modulus for optical glass fiber has been found to vary linearly with strain, according to $E = E_0(1+3\epsilon)$, for strength levels of concern in this study, where E_0 is the zero strain modulus.^{10,11} Thus, the maximum bend stress, σ_b , at $\theta=\pi/2$ only occurs along a thin line along the fiber lengths and is given by,

$$\sigma_b = E \frac{r}{R} \quad (8a)$$

Therefore, the bend stress at any point on the tensile surface is simply,

$$\sigma = \sigma_b \sin \theta \quad (8b)$$

The Weibull cumulative failure probability distribution for the case of pure bending is obtained by substituting Eq. (8b) into Eq. (2), where $dA = r d\theta$ yielding,

$$F = 1 - \exp \left[- \int_0^{\pi} \int_0^{l_b} \left(\frac{\sigma_b \sin \theta}{\sigma_o} \right)^m \frac{r d\theta d\theta}{A_o} \right] \quad (9)$$

Integrating over length l_b reduces the above equation to,

$$F = 1 - \exp \left[- \left(\frac{\sigma_b}{\sigma_o} \right)^m \frac{r l_b}{A_o} \int_0^{\pi} \sin^m \theta d\theta \right] \quad (10)$$

Following the derivation of Matthewson et. al.⁹ we let,

$$G(m) \equiv \frac{1}{2} \int_0^{\pi} \sin^m \theta d\theta = \int_0^{\frac{\pi}{2}} \sin^m \theta d\theta = \frac{\sqrt{\pi}}{2} \frac{\Gamma\left(\frac{m+1}{2}\right)}{\Gamma\left(\frac{m+2}{2}\right)} \quad (11)$$

where $\Gamma(m)$ is the gamma function which is readily determined using polynomial approximations.¹² Substitution of Eq. (11) into Eq. (10) gives the cumulative failure probability distribution for bending in terms of maximum bending stress, σ_b , and the length under bending, l_b , for a fiber of radius r.

$$F = 1 - \exp \left[- \left(\frac{\sigma_b}{\sigma_o} \right)^m \frac{2r l_b}{A_o} G(m) \right] \quad (12)$$

Thus, given σ_o and A_o from the composite 20 meter gauge length tensile distribution in Figure 8, one can calculate the failure probability for various lengths in bending. Figure 11 shows failure probability predictions for a range of bend lengths.

The predictions in Figure 11 show that, similar to the tensile distribution, the longer the bend length is, the greater the failure probability will be. However, the predicted distributions in bending show a lower failure probability for the same length and stress level than that given by tensile distributions in Figure 9. This is a consequence of the fact that bending places fewer flaws at risk than tension. The predicted distribution for 100 meter lengths in bending is shown in Figure 11 to fall on top of the original 20 meter tensile distribution. Thus, for the Weibull slopes in this data, loading 100 meters to a constant radius in bending is equivalent to loading 20 meters in tension. This will be discussed further in a later section.

In light of the bend predictions we now examine a common application that uses bending; namely, splice enclosures. The goal here is to determine that portion of the distribution which is most critical for making reliability predictions. As a worse case, we assume that in a splice enclosure 1 meter of fiber is placed in bending under a constant radius. The predicted distribution for this application is shown in Figure 11. For a failure probability requirement of 1×10^{-5} , flaws with strengths in the 150 kpsi (1050 MPa) range are expected to be encountered (note that post-proof strengths are somewhat greater than the fatigue strengths obtained in this study). For failure probabilities $< 1 \times 10^{-5}$, flaws with strengths near the proof stress level will be encountered even for 1 meter lengths in bending. When one accounts for all of the fiber in splice enclosures, such a low range of failure probabilities may not be unreasonable.

Mean strengths in Bending and Tension.

The mean strength for a distribution of the form,

$$F = 1 - \exp \left[- \left(\frac{\sigma}{\sigma'} \right)^m \right] \quad (13)$$

is given by,⁹

$$\bar{\sigma} = \sigma' \Gamma \left(1 + \frac{1}{m} \right) \quad (14)$$

Thus for the tensile distribution in Eq. (4) the mean strength is,

$$\bar{\sigma}_t = \sigma_o \left(\frac{A_o}{2\pi r l_t} \right)^{\frac{1}{m}} \Gamma \left(1 + \frac{1}{m} \right) \quad (15)$$

and similarly the mean strength for a constant bend radius from Eq. (12) is,

$$\bar{\sigma}_b = \sigma_o \left(\frac{A_o}{2r l_b G(m)} \right)^{\frac{1}{m}} \Gamma \left(1 + \frac{1}{m} \right) \quad (16)$$

The ratio of the mean strength for a fiber with a constant bend radius to mean tensile strength is then,

$$\frac{\bar{\sigma}_b}{\bar{\sigma}_t} = \sigma_o \left[\frac{\pi}{G(m)} \frac{l_t}{l_b} \right]^{\frac{1}{m}} \quad (17)$$

Thus, the mean strength in bending can be predicted given the mean tensile strength, the ratio of tensile to bend lengths and the Weibull slope parameter, m. This analysis is particularly useful since mean bend strength for a constant bend radius cannot easily be measured. Figure 12 is a plot of the ratio of mean strengths in Eq. (17) for a 20 meter tensile length and a range of bend lengths. As the Weibull slope, m, increases, i.e., variability in flaw size decreases, the difference in mean strengths decreases. For m values less than 15 the ratio of mean strengths is a strong function of the variability in flaw size.

An alternate expression for the failure probability in bending is obtained by substituting the value for σ_o in Eq. (15) into Eq. (12) giving,

$$F = 1 - \exp \left[- \left(\frac{\sigma_b}{\sigma_t} \right)^m \frac{1}{\frac{\pi}{G(m)} \frac{l_t}{l_b}} \Gamma \left(1 + \frac{1}{m} \right) \right] \quad (18)$$

Knowing the mean strength for a given tensile strength distribution and the unimodal Weibull slope, one can calculate the failure probability for a given bend stress and bend length.

Equivalent tensile length.

It is difficult to determine the flaws that are of greatest reliability risk for bending applications, due to the complexity of the stress distribution over the fiber surface. Large flaws near the neutral axis are of lower risk than small flaws at $\theta = \pi/2$. It therefore is helpful to translate the bend condition to an equivalent tensile condition.⁹

The equivalent tensile test length, l_{eq} , for a given bend length, l_b , is determined where the mean tensile strength equals the mean bend strength in Eq. (17),

$$l_{eq} = \frac{G(m)}{\pi} l_b \quad (19)$$

Equation 18 is plotted in Figures 13 and 14 for the equivalent tensile length as a function of bend length, for both long- and short-length applications, respectively. For an m value of approximately 15, the equivalent tensile length is nearly 1/10th the bend length. That is to say, a 1 kilometer length in bending is equivalent to testing 100 meters in tension. This analysis is helpful in determining the appropriate strength testing requirements for reliability prediction. For example, a bending application involving a total of 1000 kilometers requires tensile data for approximately 100 kilometers of fiber.

Summary

Long-length strength distributions are necessary for making failure predictions at very low probabilities. In this paper, a 386 kilometer strength distribution was examined in light of theoretical distributions of proof tested fibers. This distribution showed the beginnings of the classical truncated distribution associated with proof testing; however, it lacked data near the proof stress level where Weibull slopes are believed to be on the order of n. The distribution was extended to strength levels near the proof stress level in a conservative fashion using conventional Weibull statistics. This composite distribution was then scaled to a variety of lengths for both bending and tensile applications.

Even though bending only stresses 10 to 20% of the fiber surface when compared to tension, bending applications need be concerned with flaws near the proof stress level, particularly for high reliability requirements. Such analyses are needed for reliability predictions and in determining strength testing requirements for various tensile and bending applications.

References

1. K.E. Lu, G.S. Glaesemann, M.T. Lee, D.R. Powers, and J.S. Abbott, "Mechanical and Hydrogen Characteristics of Hermetically Coated Optical Fiber," Opt. Quantum Electron. 22, 227-237 (1990).
2. G.S. Glaesemann and D.J. Walter, "Method of Obtaining Long-length Strength Distributions for Reliability Prediction," Opt. Eng., 30 (6), 746-748 (1991).
3. E.R. Fuller, Jr., S.M. Wiederhorn, J.E. Ritter, Jr., P.B. Oates, "Proof Testing of Ceramics, Part 2: Theory," J. Mater. Sci., 15, 2282-2295 (1980).
4. G.S. Glaesemann and S.T. Gulati, "Dynamic Fatigue Data for Fatigue Resistant Fiber in Tension vs. Bending," in 1989 Technical Digest Series. Vol. 5, Proc Optical Fiber Communication Conference, 48 (1989).

5. G.S. Glaesemann, M.L. Elder, and J.W. Adams, "Dependence of fatigue resistance on Titania doping of silica-clad optical fiber," presented at Optical Fiber Communication Conference, post-dead paper PD 13-1 - PD13-4 (1990).

6. J.E. Ritter, Jr, N. Bandyopadhyay, and K. Jakus, "Statistical Reproducibility of the Dynamic and Static Fatigue Experiments," Amer. Ceram. Soc. Bul. 60 (8) 798 - 806 (1981).

7. W. Weibull, "Statistical Distribution Function of Wide Applicability," J. Appl. Mech., 18(3) 293-297 (1951).

8. W.D. Scott and A. Gaddipati, "Weibull Parameters and the Strength of Long Glass Fibers," in Fracture Mechanics of Ceramics, Vol. 3, edited by R.C. Bradt, D.P.H. Hasselman and F.F. Lange (Plenum Press, New York, 1978) pp. 125-42.

9. M.J. Matthewson, C.R. Kurkjian, and S.T. Gulati, "Strength Measurement of Optical Fibers by Bending," J. Am. Ceram. Soc., 69 (11) 815-821 (1986).

10. G. S. Glaesemann, S. T. Gulati, and J. D. Helfinstine, "The Effect of Strain and Surface Composition on Young's Modulus of Optical Fibers", Optical Fiber Communication Conference, 1988 Technical Digest Series, Vol.1 (Optical Society of America, Washington, DC 1988), p.26.

11. J.T. Krause, L.R. Testardi, and R.N. Thurston, "Deviations from Linearity in the Dependence of Elongation upon Force for Fibers of Simple Glass Formers and of Glass Optical Lightguides," Phys. Chem. Glasses 20(6) 135-139 (1979)

12. M. Abramowitz and I.A. Stegun, Handbook of Mathematical Functions. Dover, New York, 1964.

Figure 1.
Strength Distribution of Standard Silica-Clad Fiber

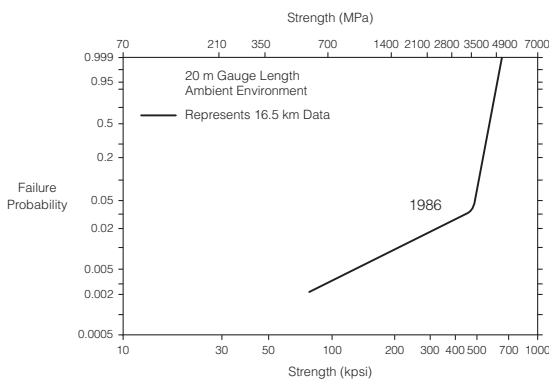


Figure 2.
If Every 20 m Specimen Stressed to Only 400 kpsi (2800 MPa)

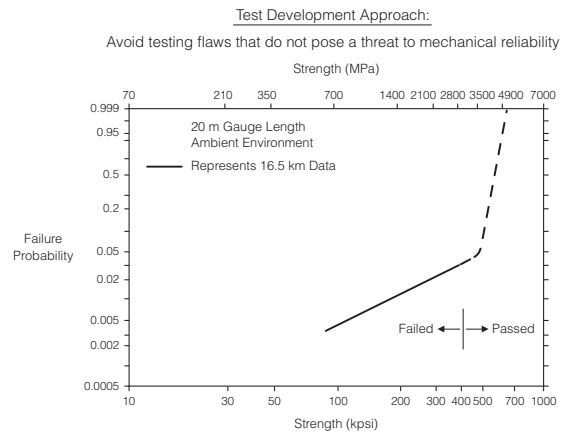


Figure 3.
Schematic of Continuous Fiber Strength Test Apparatus

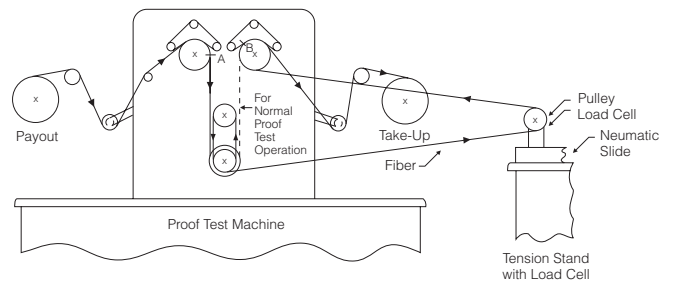


Figure 4.
Loading Cycle of 20 Meter Gauge Length

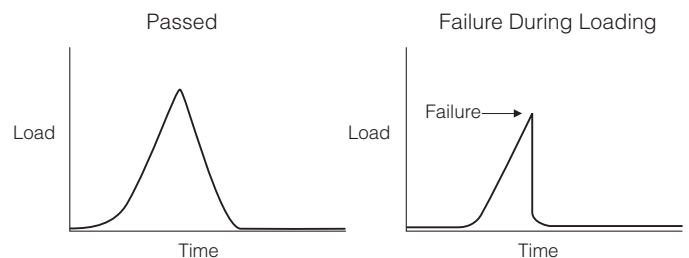


Figure 5.
Strength Distribution of 386 Kilometers of
Titania-Doped Silica-Clad Fiber

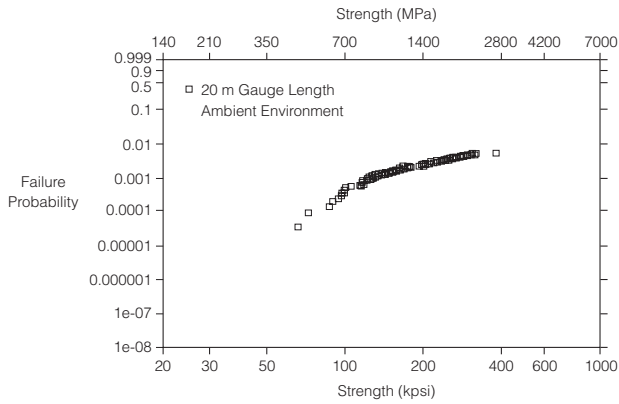


Figure 6.
Theoretical Strength Distribution after Proof Testing
Reference 3.

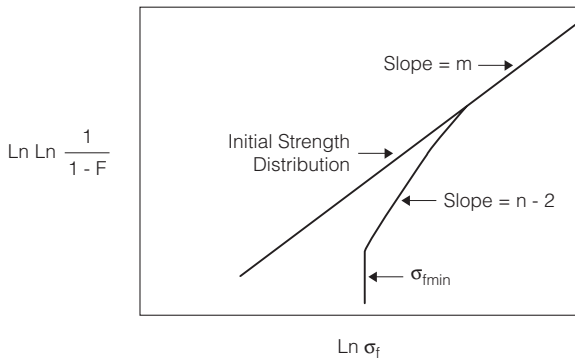


Figure 7.
Cross-Section of Fiber

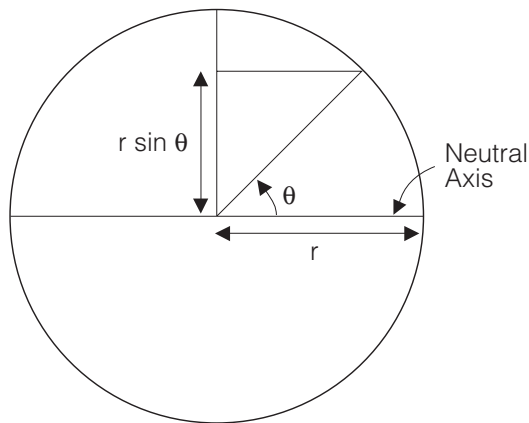


Figure 8.
Composite Long-Length Strength Distribution

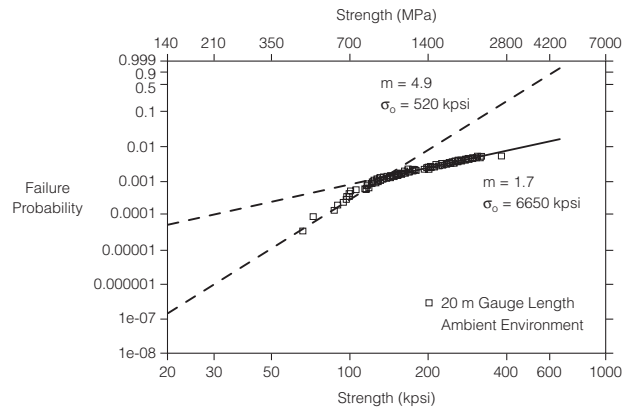


Figure 9.
Failure Probability Predictions for Tension

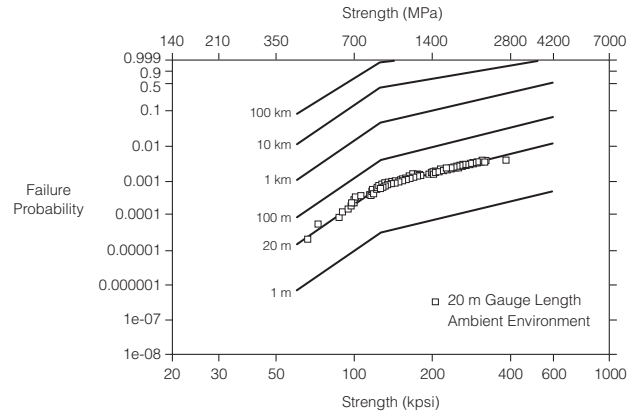


Figure 10.
Fiber in Bending

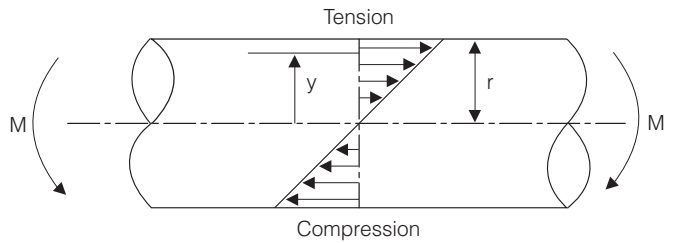


Figure 11.
Failure Probability Predictions for Bending

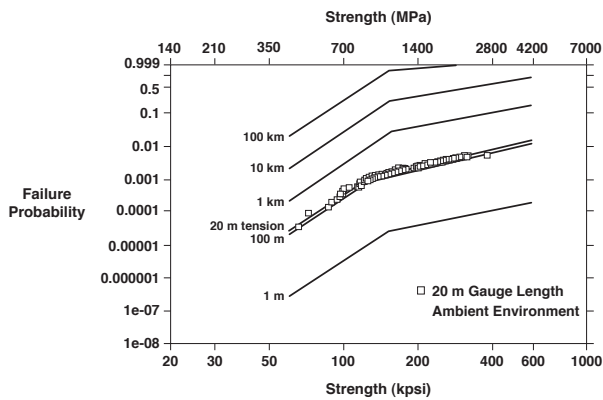


Figure 14.
Equivalent Tensile Test Length for Bent Fiber Short-Lengths

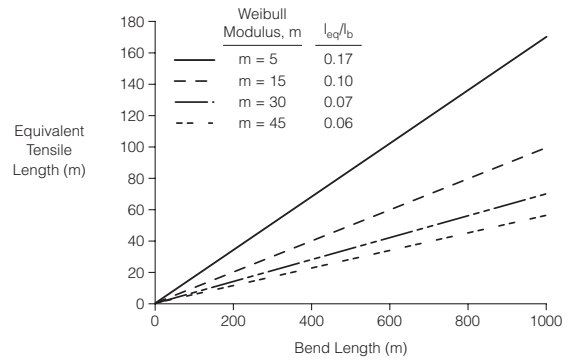
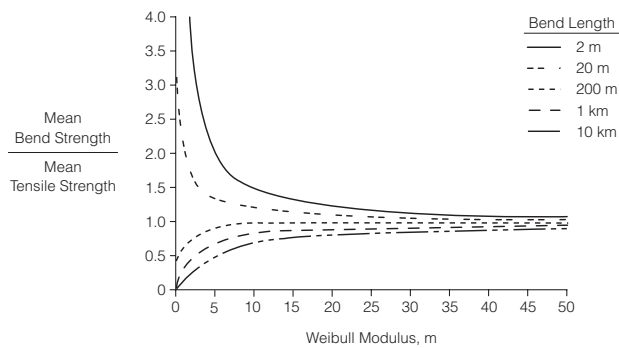


Figure 12.
Predicted Mean Bend Strength
20 Meter Tensile Measurement



G. Scott Glaesemann, SP-DV-01-8 Corning Inc., Corning, N.Y., 14831. Glaesemann is a senior development engineer responsible for the optical waveguide strength laboratory at Corning. He has been employed by Corning for five years at the Sullivan Park research and development facility. Glaesemann received his master's degree and Ph. D. in mechanical engineering from the University of Massachusetts and a B. S. in mechanical engineering from North Dakota State University. He is a member of the American Ceramic Society.

Figure 13.
Equivalent Tensile Test Length for Bent Fiber Long-Lengths

